[redacted]

NASA TECHNICAL MEMORANDUM

NASA TM X-991

NASA TM X-991

WIND-TUNNEL INVESTIGATION OF DRAG AND STABILITY OF PARACHUTES AT SUPERSONIC SPEEDS

by Nickolai Charczenko

Langley Research Center
Langley Station, Hampton, Va.

NATIONAL AERONAUTICS AND SPACE ADMINISTRATION • WASHINGTON, D. C. • AUGUST 1964

[redacted]

WIND-TUNNEL INVESTIGATION OF DRAG AND STABILITY OF PARACHUTES AT SUPERSONIC SPEEDS

By Nickolai Charczenko

Langley Research Center
Langley Station, Hampton, Va.

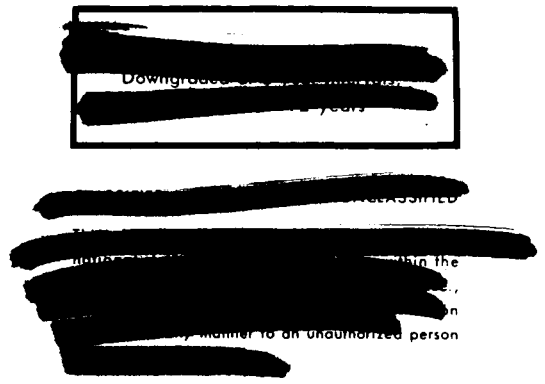

NATIONAL AERONAUTICS AND SPACE ADMINISTRATION

WIND-TUNNEL INVESTIGATION OF DRAG AND STABILITY OF PARACHUTES AT SUPERSONIC SPEEDS*

By Nickolai Charczenko
Langley Research Center

SUMMARY

An investigation has been made in the Langley Unitary Plan wind tunnel to determine drag and stability characteristics of flat-roof conical-inlet parachutes at Mach numbers from 2.30 to 4.65. The results are compared with those for conventional ribbon-type parachutes and with those for other drag devices.

The flat-roof conical-inlet parachutes provided large improvement in drag and stability over conventional ribbon-type parachutes in the test Mach number range. Larger values of drag resulted from the use of shroud lines equal in length to 2 parachute diameters as compared with values obtained with shroud lines equal to 1 parachute diameter. Fluctuating drag loads due to a change in shape and position of the shock wave existed for all parachutes and under all testing conditions.

INTRODUCTION

Conventional parachutes have, for many years, proved to be very reliable as auxiliary landing brakes for high-speed aircraft and as subsonic decelerators for a variety of missions, such as personnel recovery and dropping of cargo or military supplies. Therefore, when the need arose for aerodynamic decelerators at supersonic speeds, particularly for the national space effort, attention was once more focused on conventional parachutes. First attempts to use parachutes for supersonic deceleration were unsuccessful primarily because of the use of low-porosity canopy configurations which caused the parachutes to be unstable. (See ref. 1.) However, the change to ribbon canopies with considerably higher porosity resulted in extension of the stable characteristics into the low supersonic speed regime (refs. 2, 3, and 4). These parachutes, with canopy porosities between 20 and 30 percent, generally had good performance characteristics up to a Mach number of about 2.0. More recent data on high-porosity ribbon-canopy parachutes have extended the stable Mach number range beyond 2; however, in this higher range the canopies were semicollapsed, a condition that resulted in relatively low drag coefficients and rather violent ribbon flutter which could cause premature failure of the parachute.

---

*Title, Unclassified.

During this period of parachute development, investigations were performed on other types of drag devices (refs. 5 to 11), and many of these devices show promise on the basis of drag and stability. From the weight and packageability standpoint, however, these devices are somewhat less desirable than parachutes.

More recently, research on parachute configurations (refs. 12 and 13) resulted in flat-roof conical-inlet configurations that show promise of not only extending the stable Mach number range for parachutes but also increasing the drag considerably. Accordingly, a number of parachutes of this type have been designed and tested and the results are presented herein. Some of the geometric variables include inlet diameter, maximum diameter, cone angle, length of shroud lines, and porosity. For comparison, tests were also made on a typical ribbon parachute. The tests were performed in the Langley Unitary Plan wind tunnel at Mach numbers from 2.30 to 4.65.

SYMBOLS

C_D	drag coefficient, $\frac{\text{Drag}}{qS}$
d	payload base diameter, in.
d_i	parachute canopy inlet diameter, in.
d_{max}	maximum constructed diameter of parachute, in.
d_1	inner vent diameter, in.
d_2	outer vent diameter, in.
l	shroud-line length, in.
M	Mach number
n	number of shroud lines
q	free-stream dynamic pressure, lb/sq ft
S	maximum design frontal area
x	distance from base of payload to inlet of parachute canopy
x/d	trailing distance in terms of payload base diameter
λ_r	canopy roof porosity
λ_i	canopy inlet porosity

λ_t total porosity of canopy

θ_e canopy roof half-angle, deg

θ_i canopy inlet half-angle, deg

APPARATUS AND MODELS

The investigation was conducted in the high Mach number test section of the Langley Unitary Plan wind tunnel, which is a variable-pressure return-flow tunnel. The test section is 4 feet square and approximately 7 feet long. The nozzle leading to the test section is an asymmetric sliding-block-type nozzle which allows the Mach number to be varied continuously from about 2.30 to 4.65. Further details of the wind tunnel may be found in reference 14.

The sketch and photographs of figure 1 show the parachute installation in the test section. A cylindrical body (payload) 2.38 inches in diameter and approximately 26 inches long was supported in the center of the tunnel by two thin struts spanning the tunnel in the horizontal plane. The struts taper both in planform and thickness from a chord of 8 inches and thickness 0.5 inch at the tunnel wall to a chord of 4 inches and thickness of 0.25 inch at the tunnel center line. The cylindrical body contained an internal strain-gage balance to which a motor-driven drum was attached as shown in figure 2. This drum was remotely operated and provided variation in riser-line length during the tests.

The output from the internal strain-gage balance, which measured the drag of the parachute, was recorded on an oscillograph recorder and a servomechanism. In addition to the instrumentation providing the drag data, a high-speed motion-picture camera (above 1,000 frames per sec) was used to provide schlieren photographs at each test condition.

The parachute models used in this investigation are shown in figure 3 and their pertinent geometric parameters and construction materials are presented in table I. The parachute models with the exception of model E had a low-porosity conical-inlet canopy with a flat roof. Parachute models designated A1, A2, A3, and A4 have a conical-inlet canopy inclined 10° to the horizontal (fig. 3(a)). The roof of each canopy was designed with a low-porosity center ring encompassed by high-porosity (35 percent or 45 percent) annular perlon mesh with a narrow low-porosity circular band at the periphery of the roof. Length of shroud line, parachute diameter, and roof porosity were varied for this type of parachute. The B1 parachute differed from the A parachutes in roof construction - that is, the entire roof was made of the high-porosity perlon mesh. The B2 parachute was similar in construction to the B1 parachute; it had a very low-porosity cloth roof with a 1-inch center vent. The canopy inlet of this parachute was inclined 20° to the horizontal. The B parachute models are shown in figure 3(b). The D parachutes had ribbon roofs which differed slightly in construction; details of the D1 and D2 models are shown in figures 3(c) and 3(d), respectively. The C parachute (fig. 3(e)) had a biconic canopy and a high-porosity roof.

The E parachute was a conventional ribbon parachute with 210° hemispherical gores and a 10 percent extended skirt. (See ref. 15, p. 89.) Construction details of this model are shown in figure 3(f).

TESTS AND ACCURACIES

Test conditions for each of the parachute configurations are given in the following table:

Mach number	Dynamic pressure, lb/sq ft	Reynolds number per foot	Model
2.30	196	0.88×10^6	A1
2.30	214	.94	B1, D2, E
2.50	117	.54	A3
2.50	185	.85	A2, B1
2.50	220	1.01	A3
2.75	137	.67	A1
2.75	152	.75	A2, A4, B1, D2, E
2.75	160	.79	A3
2.90	134	.65	B1
3.00	124	.65	A1, A2, A3, A4, B1, B2, C, D2, E
3.00	79	.41	A3
3.20	104	.58	A1, A2, A3, A4, B1, B2, C, D2, E
3.50	81	.50	A1, A2, A3, A4, B1, B2, C, D2, E
3.75	66	.44	A1, A2, A3, A4, B1, B2, C, D2
3.75	79	.53	D1
3.75	143	.96	D1
4.00	159	1.10	A1, A3, B1
4.30	148	1.15	A3, B1
4.65	157	1.36	A3, B1

At each of the test conditions at least two drag-force data points were obtained and these were averaged in computing the drag coefficient. Drag variation with time was also obtained by using the oscillograph recorder. The riser-line length was determined approximately during the test and was more accurately measured from the schlieren motion pictures. For most of the tests the parachutes were packed in a bag and deployed after the tunnel was started.

The accuracy of individual quantities is estimated to be within the following limits:

C_D 0.02
x, in. 0.5

M = 2.30 to 3.75 . . . . . 0.015
M = 4.00 to 4.65 . . . . . 0.05

RESULTS AND DISCUSSION

Drag-Coefficient Data

The basic drag-coefficient data as a function of trailing distance are shown in figure 4 for all the test parachutes and are cross-plotted as a function of Mach number in figure 5. The results shown in figure 5 indicate that the effect of trailing distance on drag is dependent upon Mach number (see parachute A3, for example) with the effect actually reversing over the Mach number range depending upon the flow field in which the parachute is operating. With figure 5 a comparison can be made between the flat-roof conical-inlet A parachutes and parachute E which is representative of a conventional, ribbon-type, supersonic parachute. Parachutes A1, A3, and A4 produce values of drag coefficient that are extremely high when compared with those obtained for parachute E. Decreasing the shroud-line length from 16 inches or 2 parachute diameters (parachute A1) to 8 inches or 1 parachute diameter (parachute A2) leads to a severe reduction in drag coefficient at all test Mach numbers.

In an attempt to determine the reason for this large reduction in drag coefficient, a comparison was made of the high-speed schlieren motion pictures for parachutes A1 and A2. These motion pictures revealed that the bow wave in front of parachute A1 fluctuated back and forth but generally remained as a detached shock in front of the canopy. On the other hand, the bow wave in front of parachute A2 moved forward and because of the short shroud-line length became an attached shock wave at the confluence point of the shroud lines where the shock generally remained. The drag coefficient was less behind the oblique shock wave than behind a normal shock wave because of reduced dynamic pressure. As a secondary effect, the shorter shroud lines led to increased canopy breathing, also observed in references 1 and 4, which serves to reduce the drag coefficient.

An indication of the effect of the relative size of the parachute with respect to the payload can be seen in figure 5 by comparing a 6-inch-diameter parachute (A3) and an 8-inch-diameter parachute (A1). This comparison does not show any large differences in drag coefficients such as were observed with the rigid decelerators in reference 5. The drag efficiency for parachutes, unlike the drag efficiency of rigid decelerators, could remain the same with a decrease in the ratio of parachute diameter to payload base diameter. This characteristic results from a fundamental difference between parachutes and solid decelerators, namely, that parachutes function as inlets with the drag being dependent on the inlet flow conditions. Drag values of the B1 parachute which has an evenly distributed high-porosity roof and of the D2 parachute which has the ribbon roof compare reasonably well with the annular venting arrangement used on the A3 parachute. (See fig. 5.) The low drag of the B2 parachute could not be attributed to any single factor inasmuch as several parameters which could have contributed to low drag were changed. This parachute had short shroud lines,

low canopy porosity, and a larger canopy inlet angle. The combination of these parameters led to breathing and very poor inflation of the canopy and resulted in reduced drag.

Parachute D1 was tested at M = 3.75 only (fig. 4) and the drag coefficients obtained were about the same as those obtained for parachute D2 at the same Mach number.

Parachute C, which had a biconic canopy, was deployed at a Mach number of 3.75 and exhibited severe oscillations. The canopy roof failed in a short period of time, and with the torn roof the parachute stabilized. The basic data presented (figs. 4 and 5) are for the torn-roof condition and should not be construed as the drag characteristics of this parachute as designed.

Time-Drag Variation of Parachutes

The drag data were obtained by means of a strain-gage balance connected to a servomechanism which essentially averages out the drag for small periods of time. Because of the nature of the shock waves acting on and in the vicinity of parachutes, however, it must be recognized that considerable changes in drag must accompany the rapid changes in shock formations. The oscillograph records were taken in order to obtain some idea of the variations in drag experienced by a parachute in a supersonic stream; a typical record (for the D2 parachute) is presented as figure 6. It can be seen that basically there are two frequencies involved. The first is a high frequency of the order of 100 to 200 cycles per second. This frequency is caused by small local changes of the shock on individual shroud lines or small amounts of breathing of the canopy which does not predominately influence the drag level of the parachute. The lower frequencies of the order of 10 to 20 cycles per second are caused by large changes in the shock formation such as the change from a bow shock to one that is attached at the shroud line confluence point. The larger amplitudes correspond to the bow shock nearer the canopy inlet. These fluctuating drag loads could be a problem as is indicated by failure of some parachutes. Even though most parachutes stayed in the wind tunnel for many hours without showing any damage, the failure of the shroud lines of parachute A1 and partial failure of the roof of parachute A4 after only a few hours of operation are believed to be due primarily to fluctuating drag loads.

Parachute Stability Observations

The overall stability of the flat-roof conical-inlet parachutes tested was good with generally little oscillation about the point of attachment and little canopy breathing. An outstanding feature of these parachutes was that, even though fluctuations in shock wave existed to some degree for all parachutes and under all flow conditions, the inflated canopy diameter was affected very little by these changes. Small oscillations that existed about the point of attachment, particularly for the longer trailing distances, appeared to have been induced by the swivel which was used to alleviate the twisting of the shroud lines. Rotation of the parachute was observed only in a few isolated instances. However, for parachute E, the swivel did not prevent the shroud lines from

twisting. Of the 1- and 2-parachute-diameter shroud-line lengths tested, the parachute with the longer shroud lines was the more stable configuration. For a given Mach number the stability of the parachutes appeared to be a function of trailing distance - that is, the parachutes were more stable for shorter trailing distances (approx. $x/d = 7$ to 8).

Parachute State of the Art

A comparison of the drag coefficients of some of the better flat-roof conical-inlet parachutes with those of conventional ribbon-type parachutes and other types of decelerators is presented in figure 7. These data indicate that continuing research has improved the deceleration capability of parachutes by a factor of 2 to 3 in the supersonic Mach number range to about 4.0. The results for the 80° cone with the 10-percent disk indicate a considerably higher drag coefficient for the cone compared with the drag coefficient for the best flat-roof conical-inlet parachutes. However, on the basis of weight-drag ratio and with consideration given to packageability, the parachutes may well be competitive. It is recognized that many avenues of research are still unexplored and further improvement in the drag level of parachutes may yet be obtained.

CONCLUSIONS

Results of an investigation conducted at Mach numbers from 2.30 to 4.65 on flat-roof conical-inlet parachutes indicate the following conclusions:

1. Flat-roof conical-inlet parachutes provide large improvement in drag and stability over conventional ribbon-type parachutes in the Mach number range of these tests.

2. Shroud-line length appears to be an important parameter inasmuch as large reductions in drag result from use of shroud lines equal in length to 1 parachute diameter as compared with shroud lines equal to 2 parachute diameters.

3. Fluctuating drag loads due to changing shape and position of the shock wave exist for all parachutes and under all test conditions.

Langley Research Center,
National Aeronautics and Space Administration,
Langley Station, Hampton, Va., May 1, 1964.

REFERENCES

1. Meyer, R. A.: Wind Tunnel Investigation of Conventional Types of Parachute Canopies in Supersonic Flow. WADC Tech. Rep. 58-532, AD 202856, U.S. Air Force, Dec. 1958.

2. Johnson, Clinton T.: Investigation of the Characteristics of 6-Foot Drogue-Stabilization Ribbon Parachutes at High Altitudes and Low Supersonic Speeds. NASA TM X-448, 1960.

3. Engstrom, B. A.: Performance of Trailing Aerodynamic Decelerators at High Dynamic Pressures. Part II - Phase II Test Results. WADC Tech. Rep. 58-284, Pt. II, U.S. Air Force, Jan. 1960.

4. Maynard, Julian D.: Aerodynamic Characteristics of Parachutes at Mach Numbers From 1.6 to 3. NASA TN D-752, 1961.

5. Charczenko, Nickolai: Aerodynamic Characteristics of Towed Spheres, Conical Rings, and Cones Used as Decelerators at Mach Numbers From 1.57 to 4.65. NASA TN D-1789, 1963.

6. McShera, John T., Jr.: Aerodynamic Drag and Stability Characteristics of Towed Inflatable Decelerators at Supersonic Speeds. NASA TN D-1601, 1963.

7. Charczenko, Nickolai, and McShera, John T., Jr.: Aerodynamic Characteristics of Towed Cones Used as Decelerators at Mach Numbers From 1.57 to 4.65. NASA TN D-994, 1961.

8. Coats, Jack D.: Static and Dynamic Testing of Conical Trailing Decelerators for the Pershing Re-Entry Vehicle. AEDC-TN-60-188 (Contract No. AF 40(600)-800 S/A 11(60-110)), Arnold Eng. Dev. Center, Oct. 1960.

9. Aebischer, A. C.: Investigation To Determine the Feasibility of Using Inflatable Balloon Type Drag Devices for Recovery Applications in the Transonic, Supersonic, and Hypersonic Flight Regime - Part I. Functional and Performance Demonstration. ASD-TDR-62-702, Pt. I, U.S. Air Force, Oct. 1962.

10. Alexander, W. C.: Investigation to Determine the Feasibility of Using Inflatable Balloon Type Drag Devices for Recovery Applications in the Transonic, Supersonic, and Hypersonic Flight Regime - Part II. Mach 4 to Mach 10 Feasibility Investigation. ASD-TDR-62-702, Pt. II, U.S. Air Force, Dec. 1962.

11. Nebiker, F. R.: Feasibility Study of an Inflatable Type Stabilization and Deceleration System for High-Altitude and High-Speed Recovery. WADD Tech. Rep. 60-182, U.S. Air Force, Dec. 1961.

12. Heinrich, Helmut G., and Scipio, L. Albert: Performance Characteristics of Extended Skirt Parachutes. WADC Tech. Rep. 59-562, U.S. Air Force, Oct. 1959.

13. Sims, L. W.: Analytical and Experimental Investigation of Supersonic Parachute Phenomena. ASD-TDR-62-844, U.S. Air Force, Feb. 1963.

14. Anon.: Manual for Users of the Unitary Plan Wind Tunnel Facilities of the National Advisory Committee for Aeronautics. NACA, 1956.

15. American Power Jet Co.: Performance of and Design Criteria for Deployable Aerodynamic Decelerators. ASD-TR-61-579, U.S. Air Force, Dec. 1963.

16. Berndt, Rudi J.: Supersonic Parachute Research. ASD-TDR-62-236, U.S. Air Force, May 1962.

17. Kinzy, R.: Supersonic Drag of Trailing Decelerators: NASA-Langley Tests of Rigid Types and Radioplane Parachute Models. Rep. No. PTM-404, Radioplane (Van Nuys, Calif.), Jan. 12, 1962.

TABLE I

DESCRIPTION OF PARACHUTE MODELS USED IN PRESENT INVESTIGATION

Parachute	Geometric parameters												Material			Figure	Remarks
	d_{max}, in.	d_i, in.	d_1, in.	d_2, in.	θ_i, deg	θ_e, deg	l, in.	n	λ_r	λ_1	λ_t	Ratio of exit area to inlet area	Cone	Suspension lines	Roof		
A1	8	7.2	4.3	7.25	10	90	16	12	18.0	2.0	10.5	0.27	Nylon cloth	Nylon cord	Nylon cloth, perlon mesh	3(a)	Flat-roof, conical-inlet canopy with annular venting.
A2	8	7.2	4.3	7.25	10	90	8	12	18.0	2.0	10.5	.27					
A3	6	5.4	3.0	4.8	10	90	12	12	14.8	2.0	8.1	.21					
A4	8	7.2	4.3	7.25	10	90	16	12	25.2	2.0	13.0	.34					
B1	6	5.4	---	6.0	10	90	12	12	32.2	2.0	18.0	0.42	Nylon cloth	Nylon cord	Perlon mesh	3(b)	Flat-roof, conical-inlet canopy with evenly distributed venting.
B2	8	4.25	---	---	20	90	8	12	3.0	2.0	2.3	.25			Nylon cloth	3(b)	Flat-roof, conical-inlet canopy with center vent.
C	8	5.6	---	5.9	20	45	8	12	20.6	0.0	9.2	0.50	Neoprene coated nylon	Nylon cord	Nylon mesh	3(e)	Biconic canopy with large center venting.
D1	8	7.2	---	7.2	10	90	16	12	20.0	2.0	11.0	0.36	Nylon cloth	Nylon cord	Nylon ribbon	3(c)	Flat-roof, conical-inlet canopy, ribbon roof.
D2	6	5.4	1.0	5.2	10	90	12	12	16.0	2.0	9.0	.32				3(d)	
E	8	----	---	----	--	--	16	16	----	---	25.0	0.72	----------	Nylon cord	Nylon ribbon	3(f)	Conventional ribbon parachute with extended skirt.

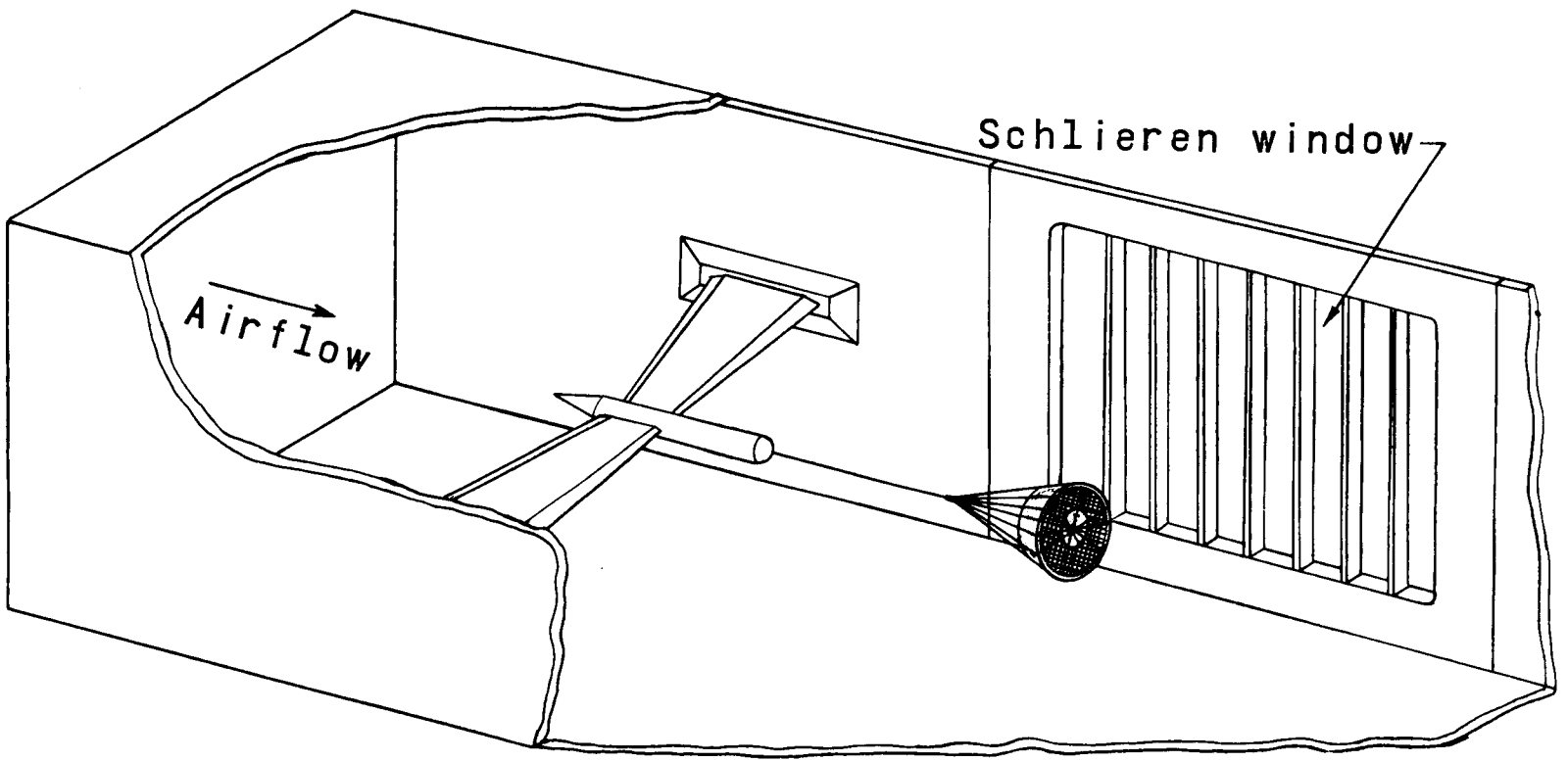

(a) Sketch of test setup.

Figure 1.- Sketch and photograph showing the test section and model installation.

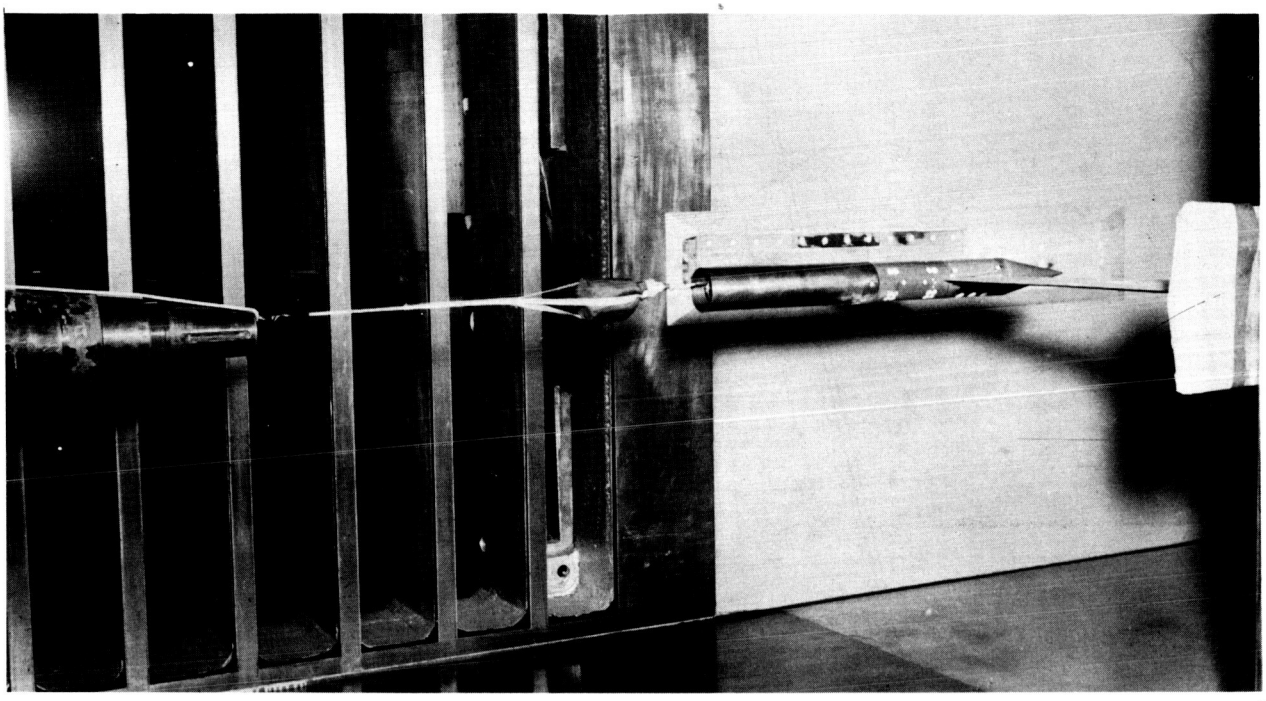

(b) Parachute packet for deployment. L-62-2696

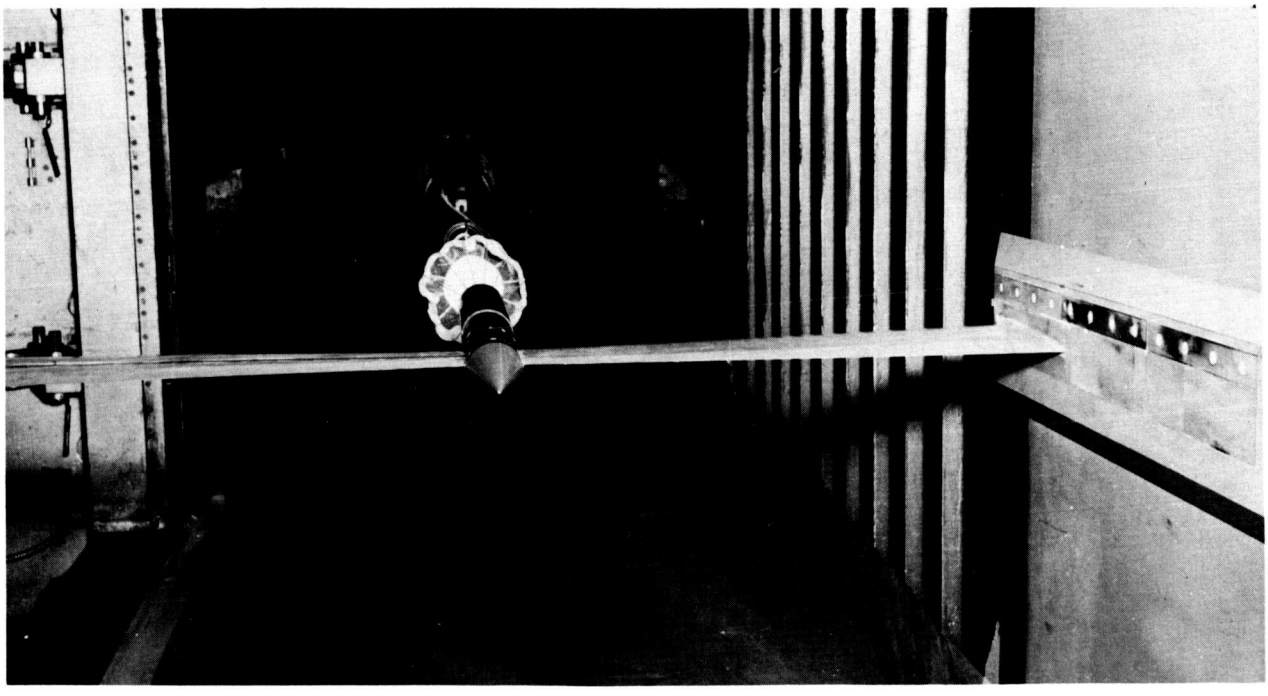

(c) Parachute A deployed. L-62-3065

Figure 1.- Concluded.

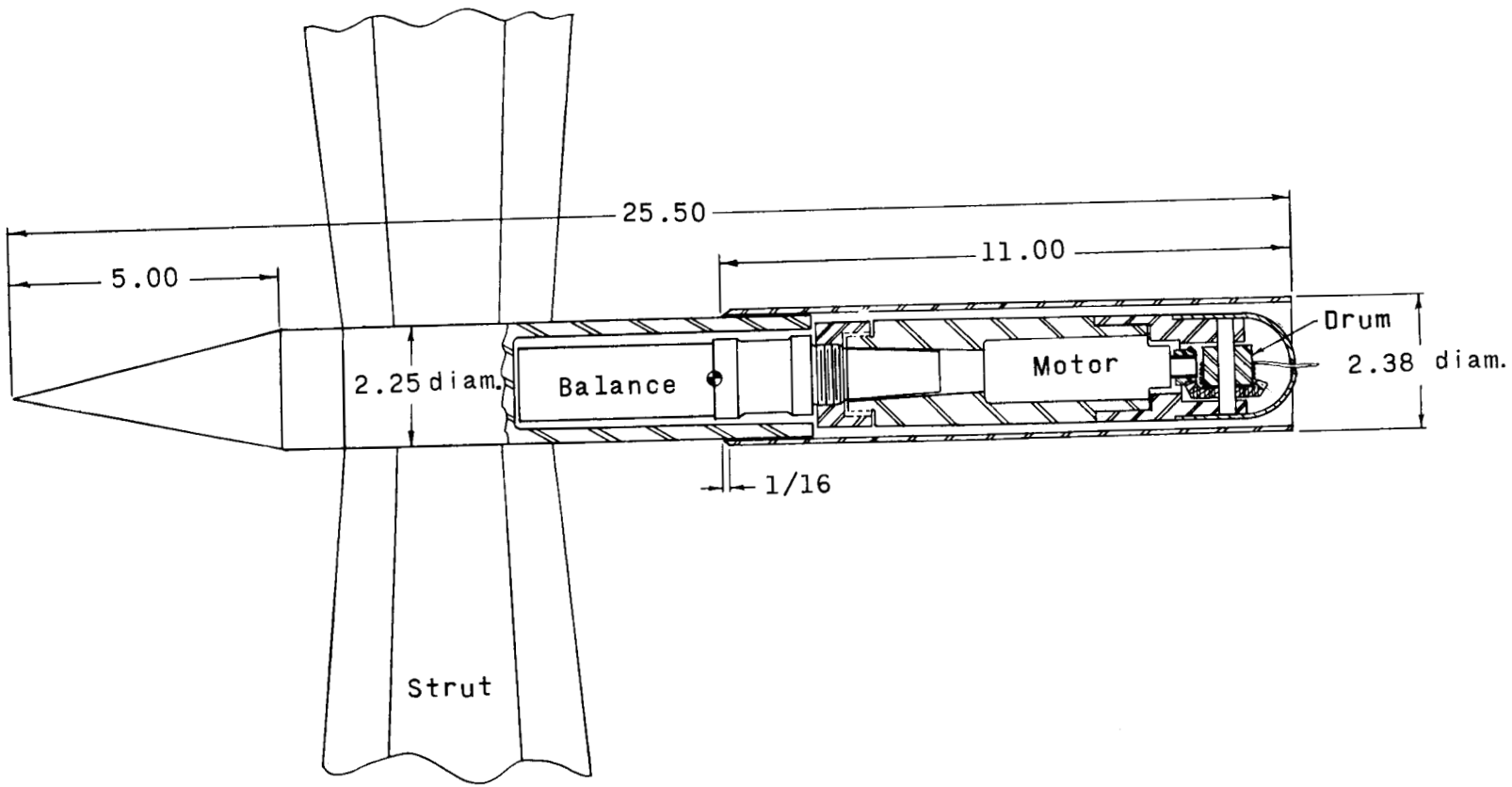

Figure 2.- Drawing of forebody with balance and motor-driven drum arrangement. All dimensions are in inches.

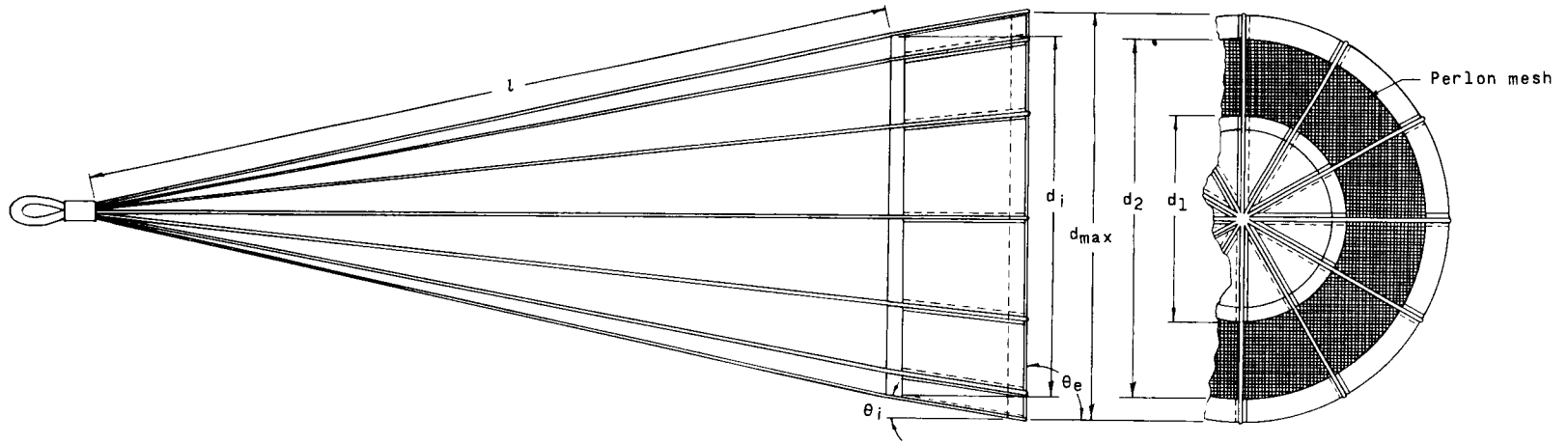

(a) Flat-roof conical-inlet canopy with high-porosity annular vent. Models A1, A2, A3, and A4.

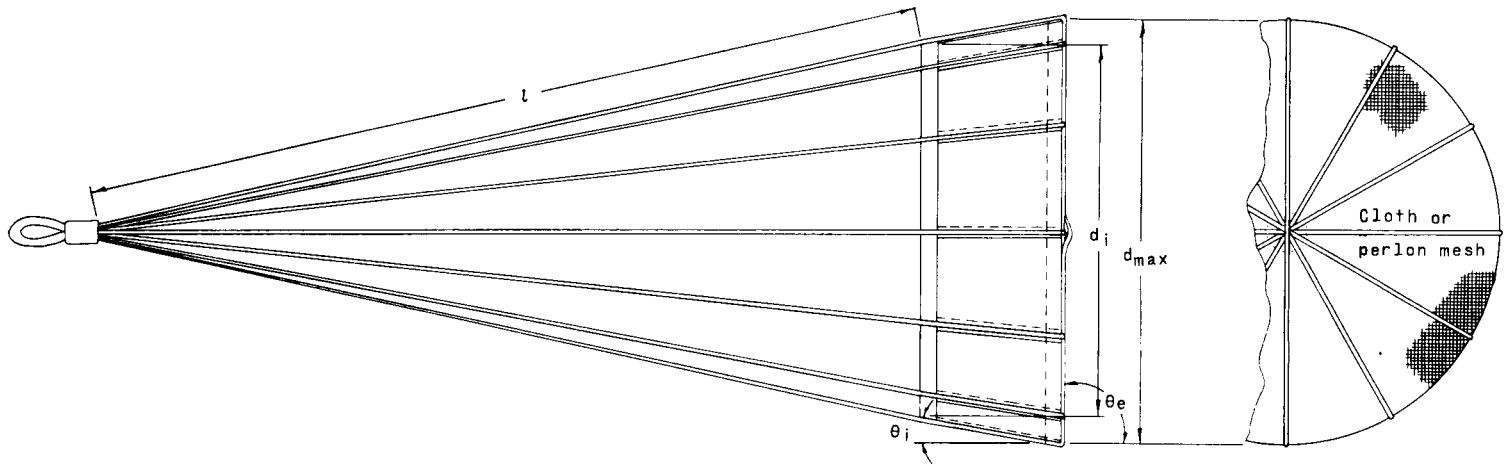

(b) Flat-roof conical-inlet canopy with cloth or perlon mesh roof. Models B1 and B2.

Figure 3.- Drawings of parachute models used in the investigation. Linear dimensions are in inches.

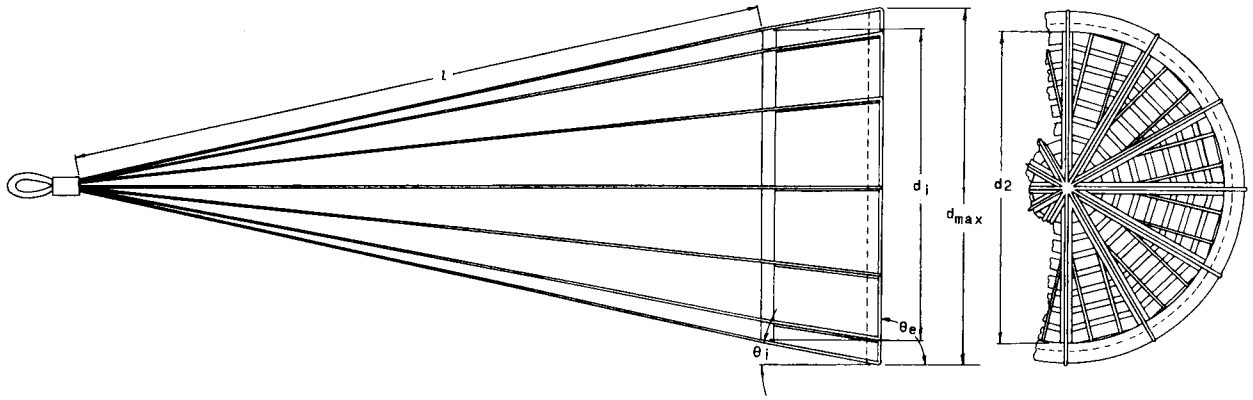

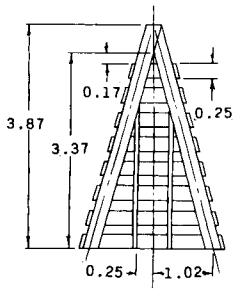

Roof gore

(c) Flat-roof conical-inlet 8-inch canopy with ribbon roof. Model D1.

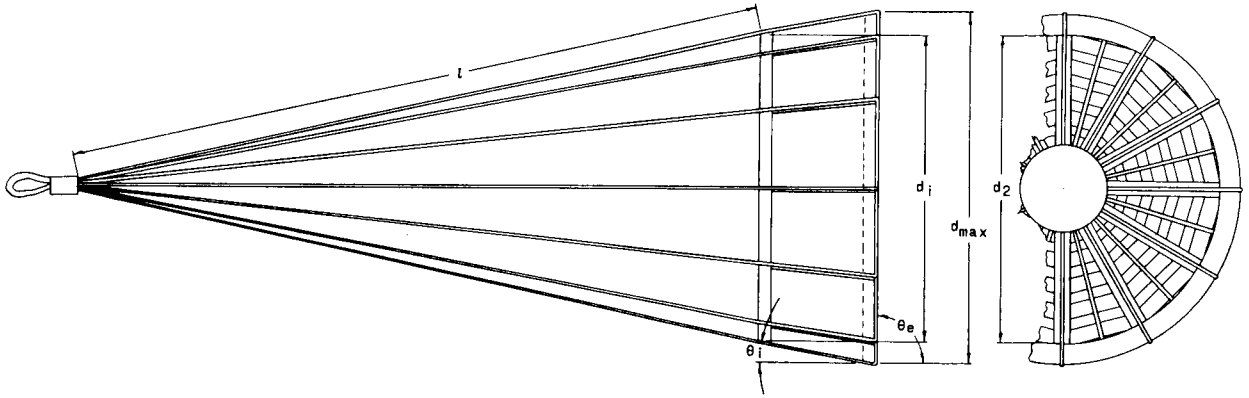

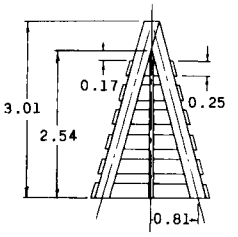

Roof gore

(d) Flat-roof conical-inlet 6-inch canopy with ribbon roof. Model D2.

Figure 3.- Continued.

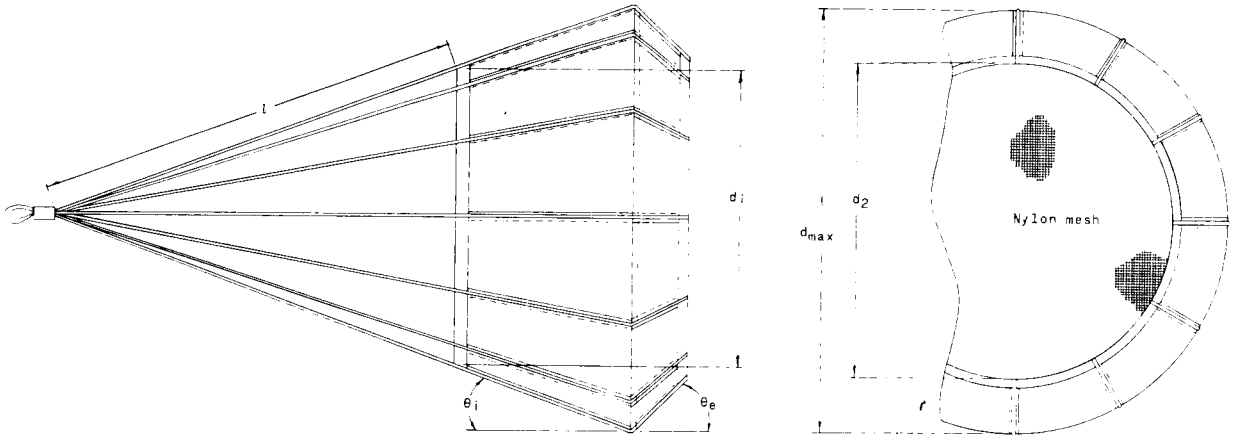

(e) Biconic canopy with high-porosity roof. Model C.

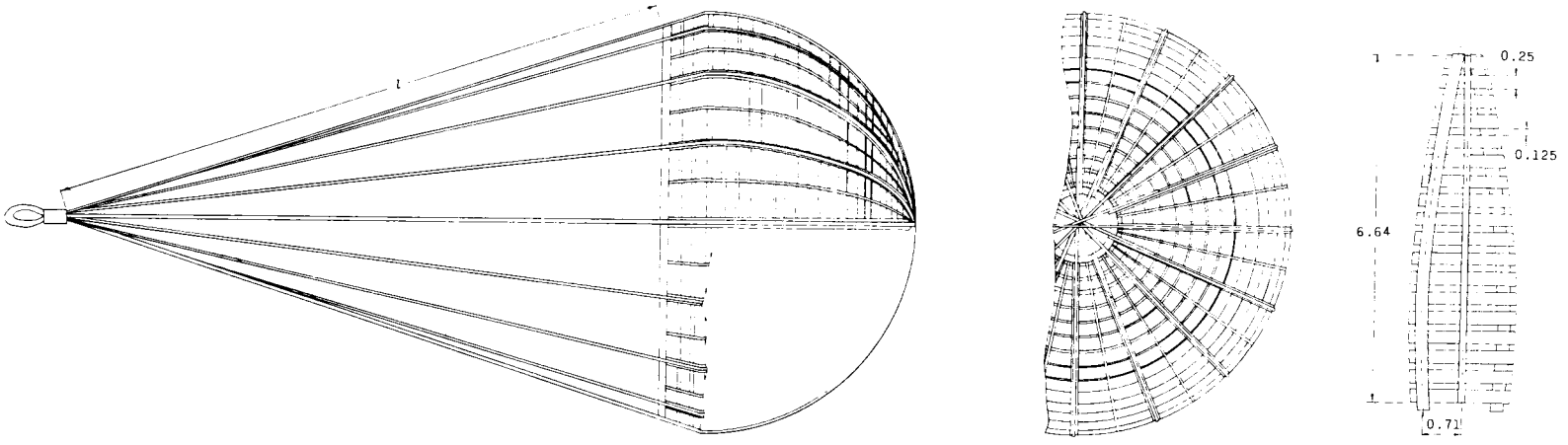

(f) Ribbon parachute with skirt. Model E.

Figure 3.- Concluded.

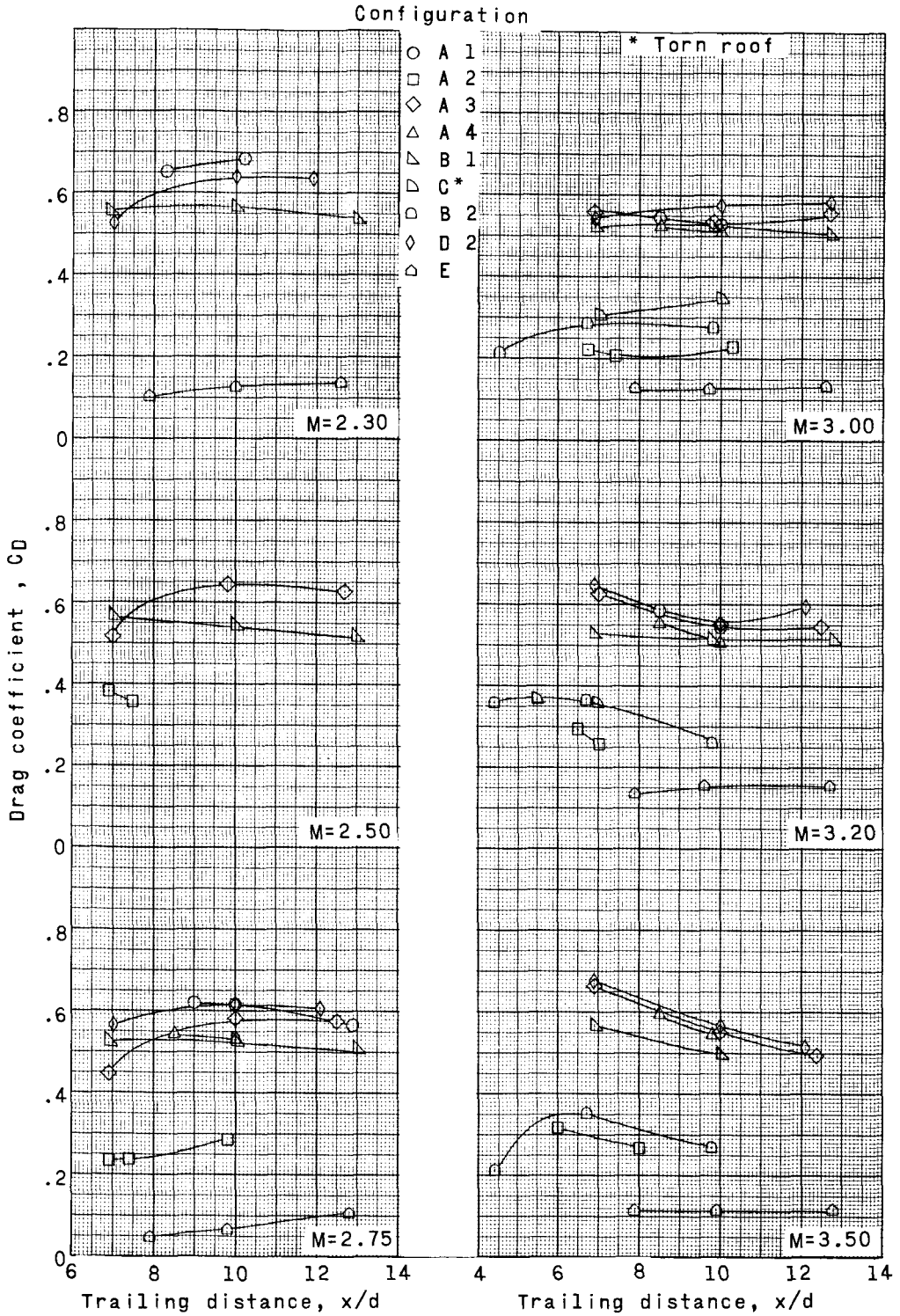

Figure 4.- Variation of drag coefficient with x/d for the parachutes tested at Mach numbers from 2.30 to 4.65.

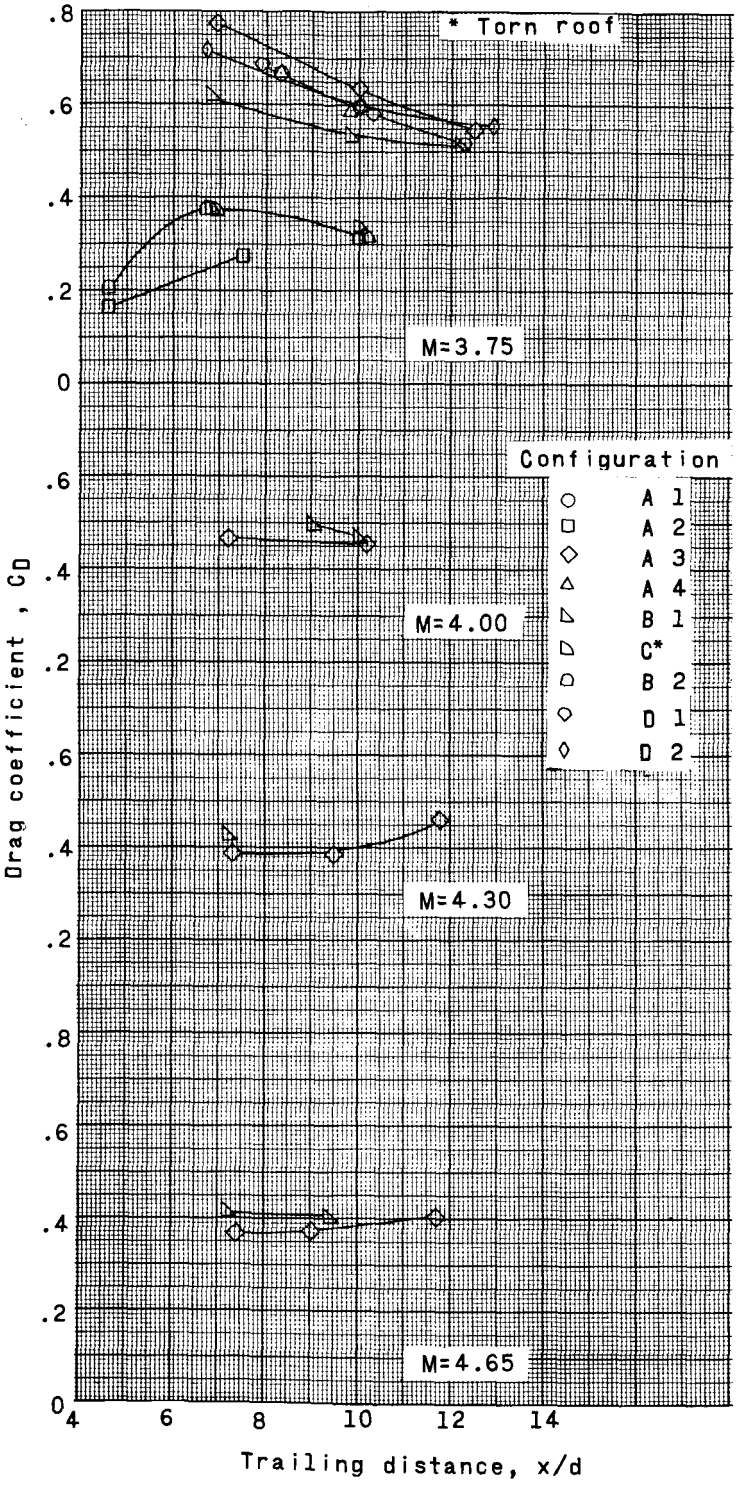

Figure 4.- Concluded.

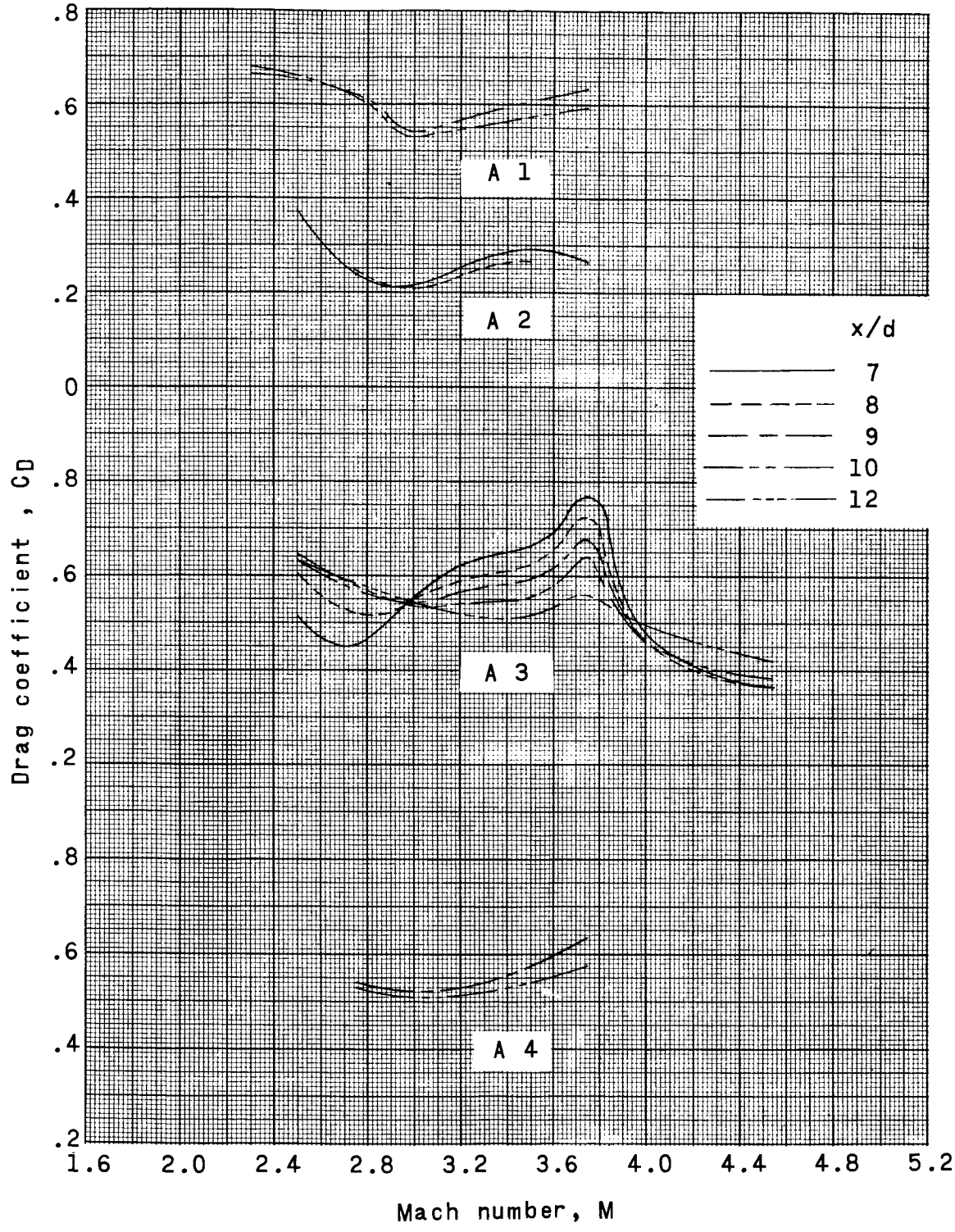

Figure 5.- Variation of drag coefficient with Mach number for various parachutes at different values of x/d.

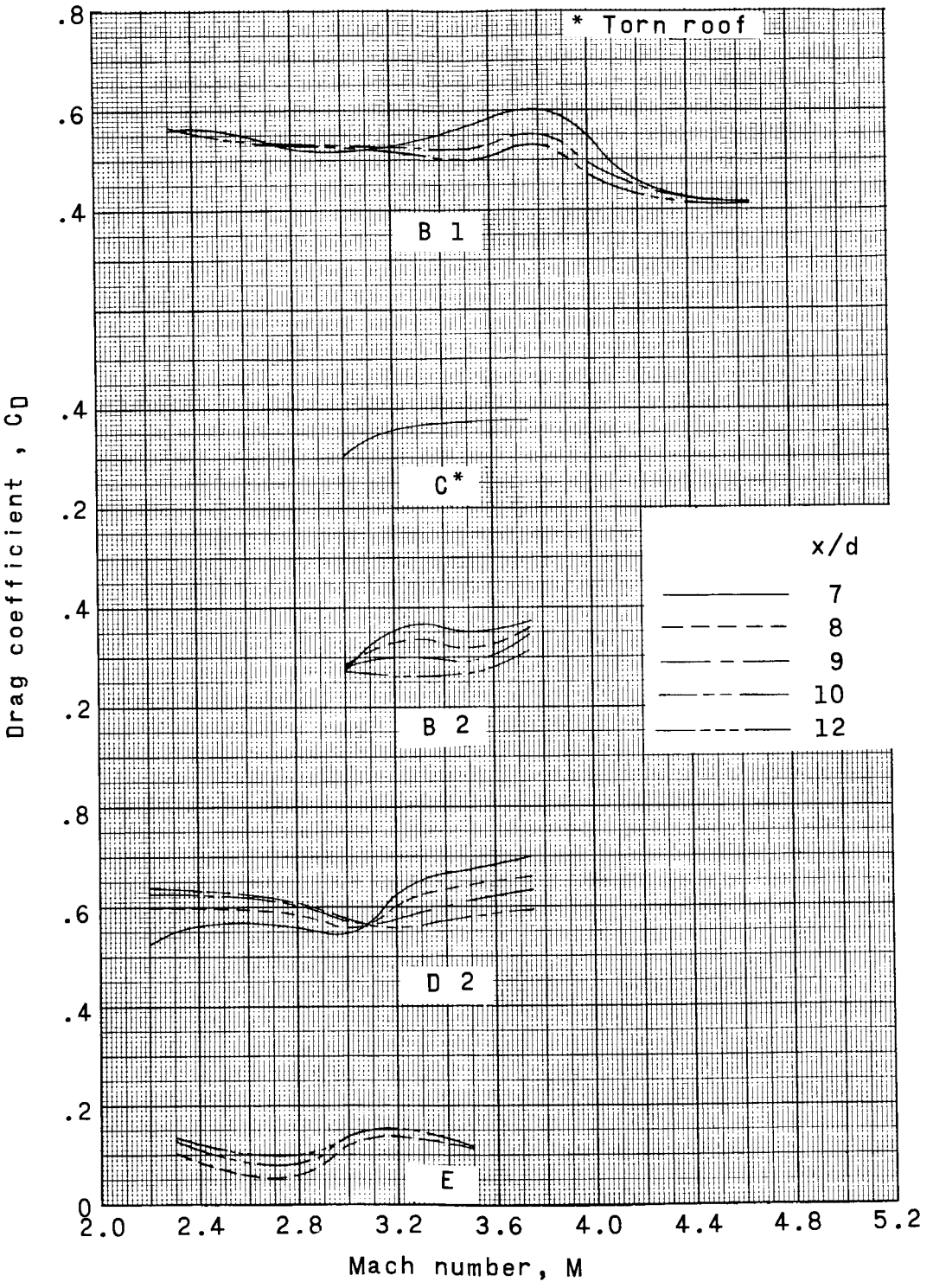

Figure 5.- Concluded.

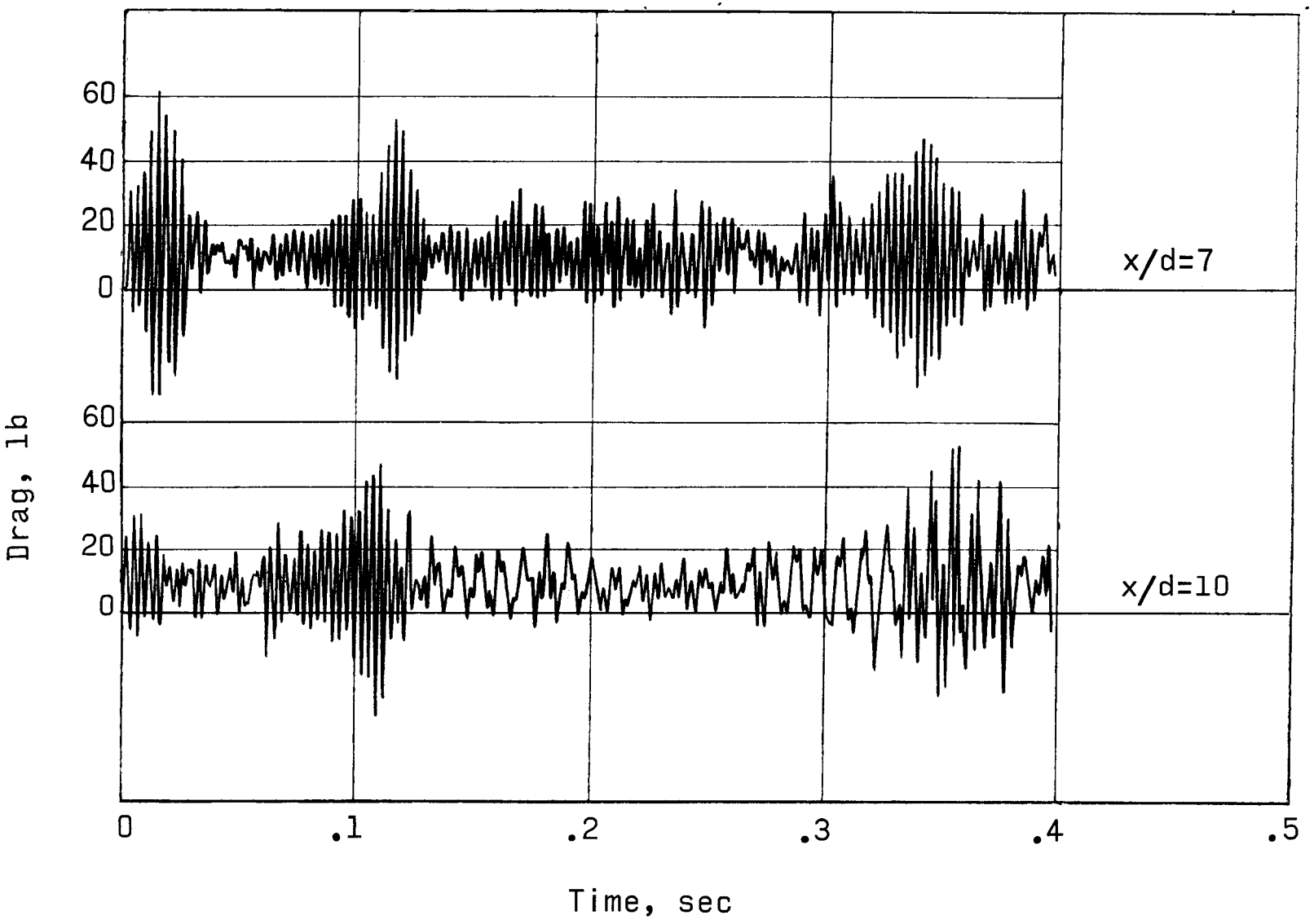

Figure 6.- Variation of drag with time for the flat-roof conical-inlet ribbon parachute (D2) at a Mach number of 3.00. q = 124 lb/sq ft.

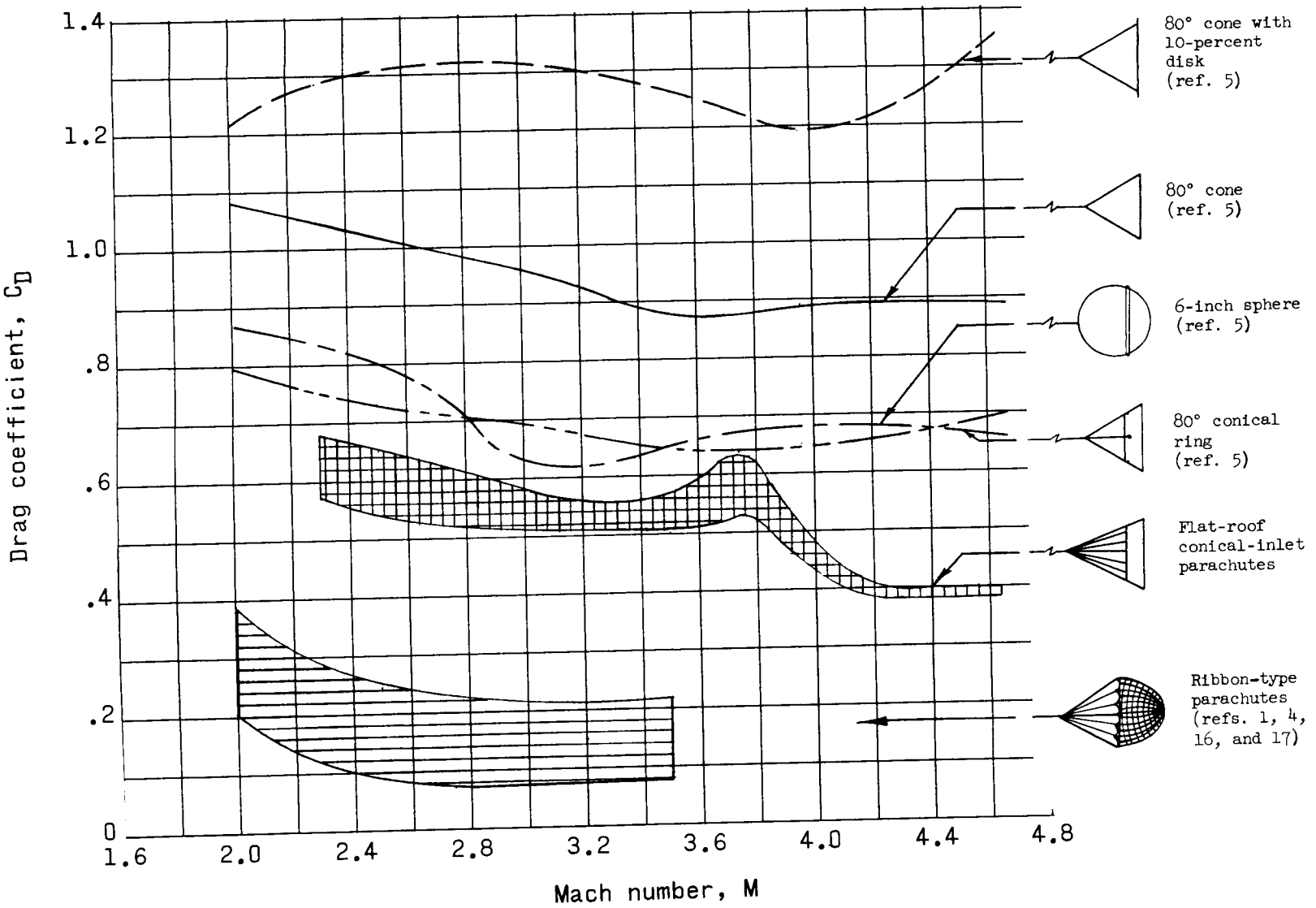

Figure 7.- Variation of drag coefficient with Mach number for various decelerators at x/d = 10.